Transient absorption spectra of the laser-dressed hydrogen atom

Mitsuko Murakami[1,*] and Shih-I Chu[1,2]

[1]*Center for Quantum Science and Engineering and Center for Advanced Study in Theoretical Sciences, Department of Physics, National Taiwan University, Taipei 10617, Taiwan*

[2]*Department of Chemistry, University of Kansas, Lawrence, Kansas 66045, USA*

(Received 2 June 2013; published 28 October 2013)

We present a theoretical study of transient absorption spectra of laser-dressed hydrogen atoms, based on numerical solutions of the time-dependent Schrödinger equation. The timing of absorption is controlled by the delay between an extreme ultra violet (XUV) pulse and an infrared (IR) laser field. The XUV pulse is isolated and several hundred attoseconds in duration, which acts as a pump to drive the ground-state electron to excited p states. The subsequent interaction with the IR field produces dressed states, which manifest as sidebands between the 1s-np absorption spectra separated by one IR-photon energy. We demonstrate that the population of dressed states is maximized when the timing of the XUV pulse coincides with the zero crossing of the IR field, and that their energies can be manipulated in a subcycle time scale by adding a chirp to the IR field. An alternative perspective to the problem is to think of the XUV pulse as a probe to detect the dynamical ac Stark shifts. Our results indicate that the accidental degeneracy of the hydrogen excited states is removed while they are dressed by the IR field, leading to large ac Stark shifts. Furthermore, we observe the Autler-Townes doublets for the $n = 2$ and 3 levels using the 656 nm dressing field, but their separation does not agree with the prediction by the conventional three-level model that neglects the dynamical ac Stark shifts.

DOI: 10.1103/PhysRevA.88.043428 PACS number(s): 32.80.Rm, 42.65.Ky

I. INTRODUCTION

Transient absorption spectra of laser-dressed atoms have been measured recently for krypton [1], argon [2], and helium [3,4]. In these experiments, an isolated XUV attosecond pulse was used to measure the subcycle change in electronic structures of the atom caused by a moderately strong ($\sim$TW cm^{-2}) IR laser field. Nonperturbative theories to account for the experimental spectra have also been developed along the way, e.g., [5–9].

In this work, the transient absorption spectra of hydrogen atoms based on numerical solutions of the time-dependent Schrödinger equation (TDSE) are studied in detail. The spectra are obtained from time-dependent dipole moments, following the method of Ref. [7]. Aside from the fundamental interest in precision spectroscopy [10], the calculation of hydrogen spectra is important because of its exactness; ground-state electronic structures are known analytically, and there is no approximation involved in numerical calculations of the TDSE. The hydrogen atom should serve as a test bed for different approaches in the theory of transient absorption spectroscopy. Absorption spectra of laser-dressed hydrogen atoms were previously studied in Ref. [11], but the timing of absorption was fixed. We present a comprehensive account for the transient absorption spectra of hydrogen atoms using various dressing-laser wavelengths and intensities.

We consider the cases where an IR field and an XUV pulse overlap in time, as shown in Fig. 1. The IR field is 12 optical cycles long, and its peak intensity is kept not so strong (1–10 TW cm^{-2}) as to induce tunneling ionizations. On the other hand, the XUV pulse is relatively weak (peak intensity: 10^{10} W cm^{-2}), and its duration is set to be two optical cycles which is about 600–800 as for various IR wavelengths considered in this work (656, 800, and 1600 nm). Such a short, isolated pulse has a broad bandwidth in the spectral domain and may induce simultaneous single-photon transitions to the many different p states in the hydrogen atom; i.e., the XUV pulse acts as a pump to drive the ground-state electron to various excited states. The subsequent interaction with the IR field produces so-called dressed states, which appear as sidebands between the 1s-np absorption spectra separated by one IR photon energy [12]. Another way to look at the same process is to think of the XUV pulse as a probe for the amount of dynamical ac Stark shifts caused by the IR field, as recently observed for helium atoms [3,4].

Our paper is organized as follows. First, numerical methods to calculate absorption spectra are described in Sec. II. Then, in Sec. III, we discuss two physical processes behind the transient absorption spectra of hydrogen atoms, namely, the Auter-Townes effect and the dynamical ac Stark effect. Analytical estimates for the Autler-Townes splitting based on the three-level model are found for reference purposes, whose method is relegated to an Appendix. Results are presented in Sec. IV. In Sec. IV A, we examine absorption spectra as functions of driving-laser intensities while fixing the timing of the XUV pulse at the peak of the IR envelope. Next, absorption spectra as functions of time delay between the XUV pulse and the IR fields are studied in Sec. IV B. Finally, in Sec. IV C, we demonstrate that energies of dressed states can be manipulated at subcycle time scale by adding a linear chirp to the IR field. Summaries and concluding remarks are given in Sec. V. Atomic units ($e = m = \hbar = 1$) are used throughout, unless indicated otherwise.

II. METHODS

A. TDSE calculation

The state of an electron $|\psi\rangle$ evolves in time according to the TDSE:

$$i\frac{\partial}{\partial t}|\psi(t)\rangle = [\mathcal{H}_0 + V(\mathbf{r},t)]|\psi(t)\rangle. \quad (1)$$

*mitsuko@phys.ntu.edu.tw

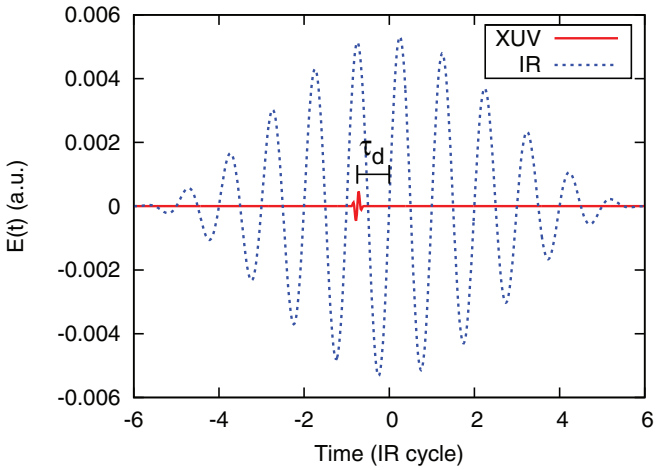

FIG. 1. (Color online) A driving laser field when the peak intensity of the IR field is 1 TW cm^{-2}.

The stationary Hamiltonian for the hydrogen atom is $\mathcal{H}_0(\mathbf{r}) = (-1/2)\nabla^2 - 1/r$. The laser-atom interaction potential in the limit of dipole approximation is given by $V(\mathbf{r},t) = -E(t)\hat{\mathbf{n}}\cdot\mathbf{r}$, where $\hat{\mathbf{n}}$ is the unit vector along the laser polarization axis. In our calculations, we take $\hat{\mathbf{n}}$ along the z axis, so that

$$V(\mathbf{r},t) = -[E_{\rm IR}(t) + E_{\rm XUV}(t-\tau_d)]z, \tag{2}$$

where τ_d is the time delay between the IR field and the XUV fields, and

$$E_{\rm IR}(t) = E_0^{\rm (IR)}(t)\sin(\omega_o t), \tag{3}$$

$$E_{\rm XUV}(t) = E_0^{\rm (XUV)}(t)\sin(q\omega_o t), \tag{4}$$

where $E_0^{\rm (XUV)}(t)$ and $E_0^{\rm (IR)}(t)$ are the pulse-envelope functions, and q is an odd integer given by $q = \lfloor I_p/\omega_o \rfloor$; this ensures the central frequency of the XUV field lies slightly below the ionization potential I_p of the atom. This definition is consistent with the experimental production of an XUV field using the high harmonic generation.

The TDSE (1) is accurately solved numerically by using the generalized pseudospectral method [13]. The maximum radius of the grid is set at $r_{\rm max} = 150$, and the absorbing boundary starts at $r_b = 100$. The time step of the evolution is $\Delta t = 0.1$. The number of collocation points along the radial coordinate is $N_r = 450$, and the maximum number of angular momentum is 18. The pulse-envelope function is $\cos^2$ shaped and centered around $t = 0$ for the IR and τ_d for the XUV, respectively. The solution $|\psi(t)\rangle$ is used to evaluate the expectation value of the time-dependent acceleration $a_z(t)$.

B. Absorption spectra

The absorption spectra are found in terms of the response function defined by [7]

$$S_+(\omega,\tau_d) = -\frac{2\omega}{t_f - \tau_d}\,{\rm Im}[\tilde{d}_z(\omega,\tau_d)\tilde{E}^*(\omega,\tau_d)] \quad (\omega > 0), \tag{5}$$

where $\tilde{d}_z(\omega) = \tilde{a}_z(\omega)/\omega^2$ is the dipole moment along the laser polarization axis, and $\tilde{E}(\omega,\tau_d)$ is the Fourier transform of the driving laser field: $E(t,\tau_d) = E_{\rm IR}(t) + E_{\rm XUV}(t-\tau_d)$. The corresponding cross section is given by

$$\sigma(\omega) = \frac{4\pi\alpha\omega S_+(\omega)}{|\tilde{E}(\omega)|^2} = \frac{8\pi\omega}{c}{\rm Im}\left[\frac{\tilde{d}_z(\omega,\tau_d)}{\tilde{E}^*(\omega,\tau_d)}\right]. \tag{6}$$

Using Beer's law, the absorption spectra can be calculated as $e^{-\sigma(\omega,\tau_d)L/2}$, where L is an interaction length [3]. We let $L = 2$ in our calculations.

The complete theoretical treatment of transient absorption spectra requires the solution of the Maxwell equation to account for the reshaping of an XUV pulse during the propagation [7]. It was found, however, that the full calculation for the helium atom yields similar results as the single-atom calculation, only scaled by the gas density [4].

III. THEORY

A. Autler-Townes effect

It is known that the $1s$-$2p$ absorption spectrum of helium atoms is split into two if they are dressed by an IR field [4]. Reference [7] gave an account for this phenomenon in terms of the three-level model as shown in Fig. 2. In this model, quasistationary states which diagonalize the Hamiltonian in the limit of the rotating wave approximation (RWA) and the adiabatic approximation $[E_0(t) \simeq E_0]$ are known as [14]

$$\begin{aligned}
|+\rangle &= \sin\Theta\sin\Phi|1\rangle + \cos\Theta\sin\Phi|2\rangle + \cos\Phi|3\rangle,\\
|-\rangle &= \sin\Theta\cos\Phi|1\rangle + \cos\Theta\cos\Phi|2\rangle - \sin\Phi|3\rangle,\\
|0\rangle &= \cos\Theta|1\rangle - \sin\Theta|3\rangle.
\end{aligned} \tag{7}$$

The mixing angles Θ and Φ are given by

$$\Theta = \tan^{-1}\left(\frac{\alpha}{\Omega}\right), \quad \Phi = \frac{1}{2}\tan^{-1}\left(\frac{\sqrt{\alpha^2+\Omega^2}}{\Delta}\right), \tag{8}$$

where α and Ω are the Rabi frequencies:

$$\Omega \equiv E_0^{\rm (IR)}\langle 2|z|3\rangle, \quad \alpha \equiv E_0^{\rm (XUV)}\langle 2|z|1\rangle, \tag{9}$$

and $\Delta \equiv (\varepsilon_2 - \varepsilon_3) - \omega_o$ is the detuning of the IR field. The corresponding (quasi) eigenvalues are

$$\varepsilon_\pm = \tfrac{1}{2}(\pm\sqrt{\alpha^2+\Omega^2+\Delta^2} \mp \Delta), \quad \varepsilon_0 = 0. \tag{10}$$

This splitting of the unperturbed energy by $\varepsilon_\pm$ is known as the Autler-Townes (AT) effect.

For the hydrogen atom, there are two possible pathways for the AT coupling of the three lowest-energy levels, as shown

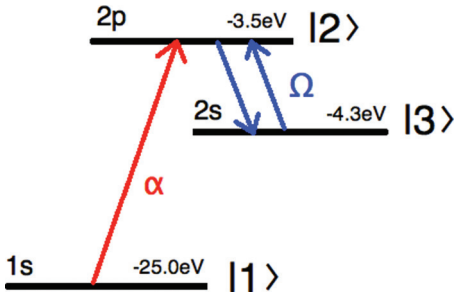

FIG. 2. (Color online) The three-level diagram of one-photon transition processes in the helium atom, driven by the broadband, isolated attosecond XUV pulse and the IR dressing field.

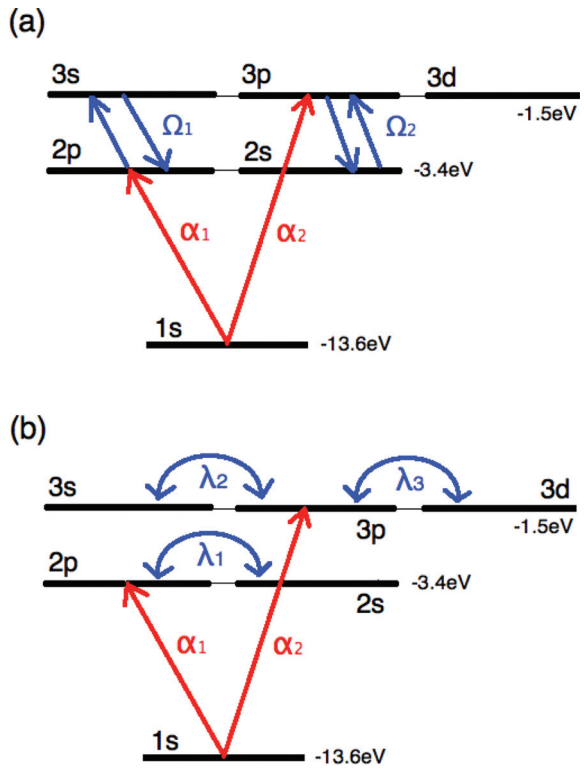

FIG. 3. (Color online) The three-level diagram of one-photon transition processes in the hydrogen atom, driven by a broadband, isolated attosecond XUV pulse and an IR dressing field. (a) If the IR-photon frequency is resonant with the transition energy between the $n = 2$ and 3 states, then there are two possible couplings to cause the Autler-Townes effect. (b) The IR field can also couple the degenerate states and alter their energies (the ac Stark effect).

in Fig. 3(a). Dipole matrix elements along the z axis for the hydrogen atom are known exactly, i.e.,

$$\begin{aligned}\langle 2p|z|1s\rangle &= \frac{2^7\sqrt{2}}{3^5} = 0.7449,\\ \langle 3p|z|1s\rangle &= \frac{3^3\sqrt{2}}{2^7} = 0.2983,\end{aligned} \tag{11}$$

$$\begin{aligned}\langle 2p|z|3s\rangle &= \frac{2^7 3^3\sqrt{6}}{5^6} = 0.5418,\\ \langle 3p|z|2s\rangle &= \frac{2^{10}3^3}{5^6} = 1.7695.\end{aligned}$$

In Table I, we list the amount of AT splittings estimated by the RWA for $\Delta = 0$, i.e.,

$$\Delta\varepsilon_i = \sqrt{{\alpha_i}^2 + {\Omega_i}^2} \quad (i = 1,2), \tag{12}$$

where $i = 1$ and 2 refers to the cascade-type transition ($1s \to 2p \to 3s$) and the λ-type transition ($1s \to 3p \to 2s$), respectively. Also shown in Table I are improved estimates based on the Floquet theory that includes the ac Stark shifts of the ground-state energies inside bichromatic fields (see the Appendix). We will refer to Table I when discussing AT splittings observed in our absorption spectra in Sec. IV.

TABLE I. The amount of Autler-Townes splitting (in the unit of eV) of the hydrogen atom for each two-photon resonance case shown in Fig. 3(a) is estimated by Eq. (12) based on the RWA, or by Eq. (A28) according to the Floquet theory that includes ac Stark shifts. The XUV intensity is 10^{10} W cm^{-2}, and the IR wavelength used for the Floquet calculation is 656 nm, in resonance with the $n = 2$ to 3 transition of the hydrogen atom. The XUV frequency is set as the seventh harmonic of the IR field.

	RWA			Floquet		
$I_0^{(\mathrm{IR})}$ (TW cm^{-2})	1	5	10	1	5	10
$\Delta\varepsilon_1^{(1s-2p)}$	0.080	0.177	0.249	0.161	0.393	0.607
$\Delta\varepsilon_2^{(1s-3p)}$	0.257	0.576	0.814	0.516	1.164	1.664

B. Dynamical ac Stark effect

Let $|n\rangle$ denote the eigenstates of the time-independent Hamiltonian $\mathcal{H}_0$, such that

$$\mathcal{H}_0|n\rangle = \varepsilon_n^{(0)}|n\rangle \quad (n = 1,2,\ldots). \tag{13}$$

The energy of $|n\rangle$ subject to a linearly polarized laser field $E(t)\hat{\mathbf{z}}$, based on the second-order time-dependent perturbation theory, is given by

$$\begin{aligned}\varepsilon_n(t) = \varepsilon_n^{(0)} &+ E(t)z_n^n\\ &- i\sum_{k\neq n}\int_0^t dt' E(t)E(t')e^{-i\omega_{kn}(t-t')}\left|z_k^n\right|^2,\end{aligned} \tag{14}$$

where $\omega_{kn} \equiv \varepsilon_k^{(0)} - \varepsilon_n^{(0)}$. If the duration of the measurement satisfies $\Delta t \gg T$, where $T \equiv 2\pi/\omega_o$ is an optical cycle of the field, then the time average of Eq. (14) is measured, i.e.,

$$\bar{\varepsilon}_n \equiv \lim_{t\to\infty}\frac{1}{t}\int_0^t \varepsilon_n(t')dt'. \tag{15}$$

The real part of the time-averaged energy is given by [15]

$$\mathrm{Re}\,\bar{\varepsilon}_n = \varepsilon_n^{(0)} - \frac{\alpha_n(\omega_o)}{4}{E_0}^2, \tag{16}$$

where E_0 is the peak value of the envelope function $E_0(t)$, and $\alpha_n(\omega_o)$ is the field polarizability:

$$\alpha_n(\omega_o) \equiv \sum_{k\neq n}\left|z_k^n\right|^2\frac{\omega_{kn}}{\omega_{kn}^2 - \omega_o^2}. \tag{17}$$

Notice that the first-order correction drops out after the time averaging. For highly excited (i.e., Rydberg) states, we have

$$\lim_{n\to\infty}\alpha_n(\omega_o) = -\frac{1}{\omega_o^2}, \tag{18}$$

which leads to the well-known upshift of ionization threshold by the ponderomotive energy: $U_p \equiv {E_0}^2/4\omega_o^2$.

In general, the term "dynamical" ac Stark effect refers to the response of the atom to the slowly varying pulse envelope $E_0(t)$ [16]. Using the XUV pulse of subfemtosecond duration as a probe, it is plausible nowadays to measure such effects. For hydrogen atoms in particular, the coupling between the degenerate states may become important while they are dressed by the IR field; this is schematically depicted in Fig. 3(b). The dipole matrix elements between such transitions

are significantly larger than the nondegenerate case:

$$\begin{aligned}\langle 2p|z|2s\rangle &= 3,\\ \langle 3p|z|3s\rangle &= 3\sqrt{6} = 7.348,\\ \langle 3d|z|3p\rangle &= 3\sqrt{3} = 5.196.\end{aligned} \tag{19}$$

The energy of the system should increase if these couplings were added, but there is no straightforward way to incorporate such effects in Eq. (14). Our calculation based on the TDSE is meant to provide a nonperturbative account for the dynamical ac Stark effect of bound electrons inside the ∼TW cm^{-2} dressing field. In principle, we can use the Floquet theory for the H atom to find exact ac Stark shifts of the bound-state energies due to the IR dressing field [17]. This will not be the same as TDSE calculations, however, as it does not incorporate the pulse envelope nor the subtle effects of an additional XUV probing field, e.g., AT splittings. Also note that the ac Stark shift is related to the ionization probability rates even at ∼TW cm^{-2} intensity levels, and thus both real and imaginary parts of the quasienergy need to be evaluated according to the Floquet theory.

If the IR laser frequency is detuned from the transition frequency, then the amount of AT splitting would diminish, according to Eq. (10). Yet, the notion of resonance in the AT effect becomes somewhat ambiguous once the atomic energy levels are altered by the dynamical ac Stark effect. Pfeiffer and Leone [8] studied the AT splitting in the high-intensity regime (where the peak IR-field intensity is in the order of 100 TW cm^{-2}) by numerically solving the three-level TDSE without the RWA. Their finding was that the inclusion of a high-frequency component in the interaction potential leads to the multiple absorption lines, rather than the doublet, and they modulate with a half-cycle periodicity of the IR field if drawn as functions of the delay time τ_d. However, their model does not include ac Stark shifts or degenerate energy levels of the hydrogen atom, and the comparison between our absorption spectra and theirs in Sec. IV B would exemplify the difference they make.

IV. RESULTS

A. Absorption spectra at the peak of the IR envelope

In Fig. 4, we plot absorption spectra as functions of peak IR-field intensities $I_0^{(\mathrm{IR})} = {E_0}^{2\,(\mathrm{IR})}$. The time delay is fixed at $\tau_d = 0$, i.e., the XUV absorptions are timed at the peak of the IR-field envelope. Results with two different IR field frequencies are shown; Fig. 4(a) is the case where the IR-photon energy is in resonance with the energy gap between the $n = 2$ and 3 states (656 nm), while Fig. 4(b) is a detuned case (800 nm). The spectra in Fig. 4(a) exhibit very clear doublets around 10.2 eV, which corresponds to the $1s$-$2p$ absorption energy. The amount of separation is about 0.5 eV at $I_0^{(\mathrm{IR})} = 2$ TW cm^{-2} and gradually increase to ∼1 eV at 10 TW cm^{-2}, which is roughly two times larger than the estimates by the Floquet theory shown in Table I. This is as expected, for the RWA or the Floquet theory assumes cycle-averaged field strengths. There are also fairly strong absorption lines at 12 and 8 eV; they represent the dressed states or, equivalently, the absorption of one IR photon by the $2p$ excited state. Their energies are downshifted as $I_0^{(\mathrm{IR})}$ increases, presumably as a result of the ac Stark effect. As the IR frequencies are detuned in Fig. 4(b), the AT doublets disappear, but the dressed states around the $1s$-$2p$ absorption line persist. In addition, multiple absorption lines appear between the $1s$-$2p$ line and its upper dressed state, and their energies are upshifted as $I_0^{(\mathrm{IR})}$ increases, suggesting yet another kind of nonperturbative ac Stark shift.

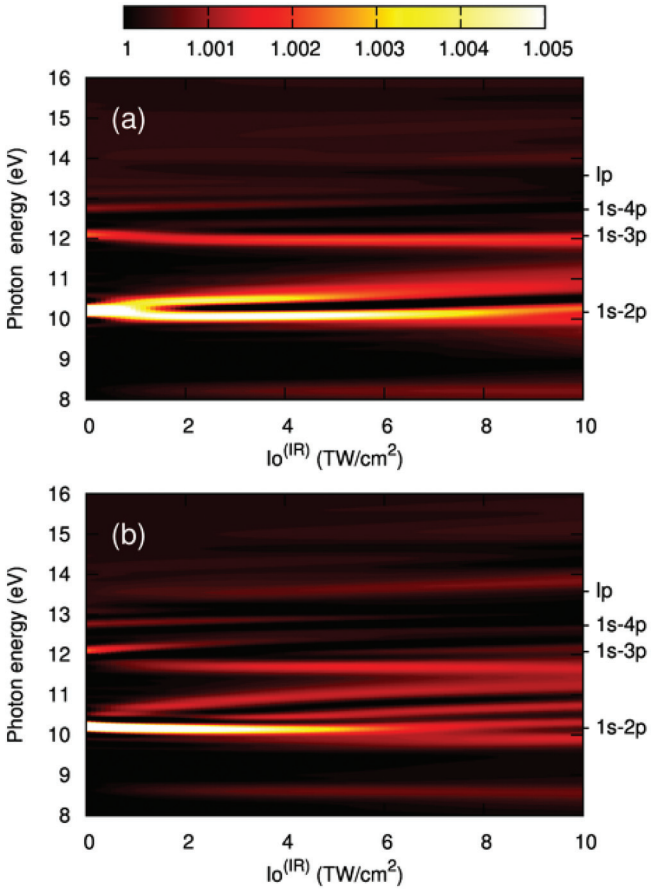

FIG. 4. (Color online) Absorption spectra of the hydrogen atom as functions of peak IR-laser intensities. The delay time of an XUV pulse is fixed at $\tau_d = 0$, and IR frequencies are (a) 656 nm (which is in resonance with the $n = 2$ to 3 transition of the hydrogen atom) and (b) 800 nm.

B. Transient absorption spectra

Next, we study absorption spectra as functions of time delay τ_d of the XUV pulse relative to the dressing IR field. Figure 5 shows absorption spectra for the 656 nm (=1.89 eV, energy difference between the $n = 2$ and 3 states) dressing field of three different peak intensities: 1, 5, and 10 TW cm^{-2}. This is a resonant case where AT doublets are expected for both $1s$-$2p$ and $1s$-$3p$ transitions, according to the three-level model pictured in Fig. 3(a). The most striking feature in Fig. 5 is the modulation of absorption lines with a period of half IR-field cycle. Closer observations of Fig. 5 reveal that the sidebands corresponding to dressed states modulate with opposite phases with the XUV absorption lines. To elucidate this point, we plot the spectra along the $1s$-$2p$ absorption energy ω_{21} and its

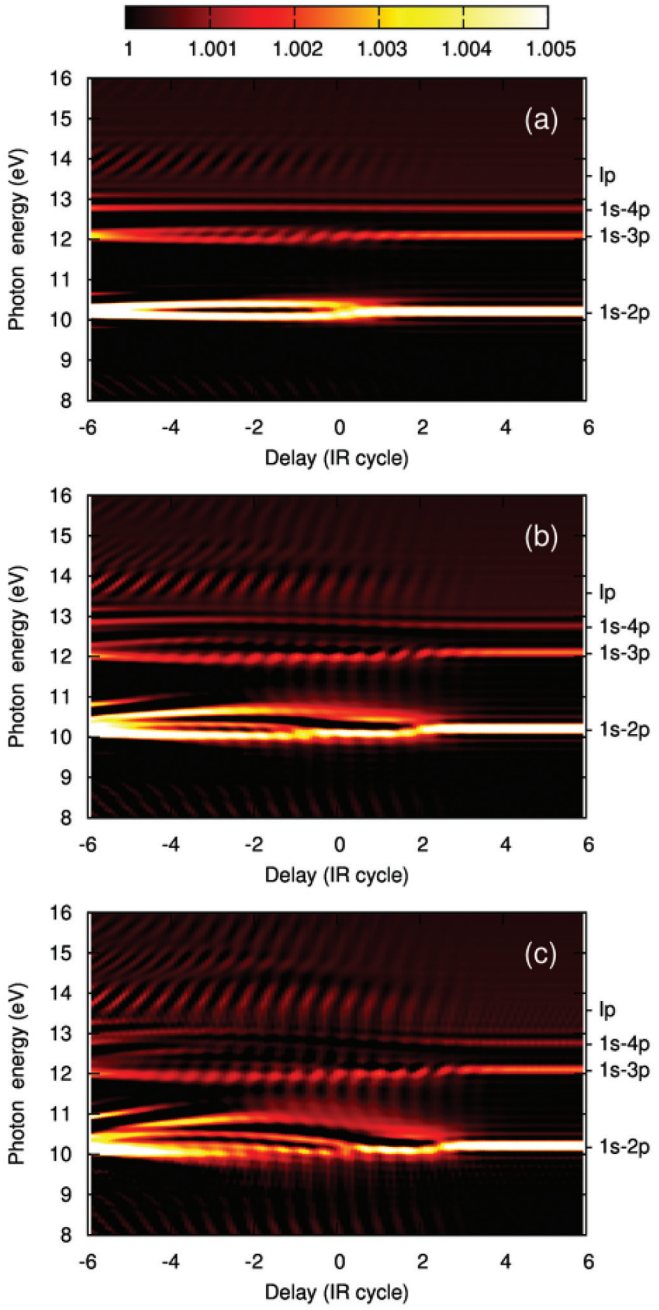

FIG. 5. (Color online) Absorption spectra of the hydrogen atom as functions of the delay time τ_d. The dressing field has the wavelength of 656 nm and peak intensities of (a) 1 TW cm^{-2}, (b) 5 TW cm^{-2}, and (c) 10 TW cm^{-2}.

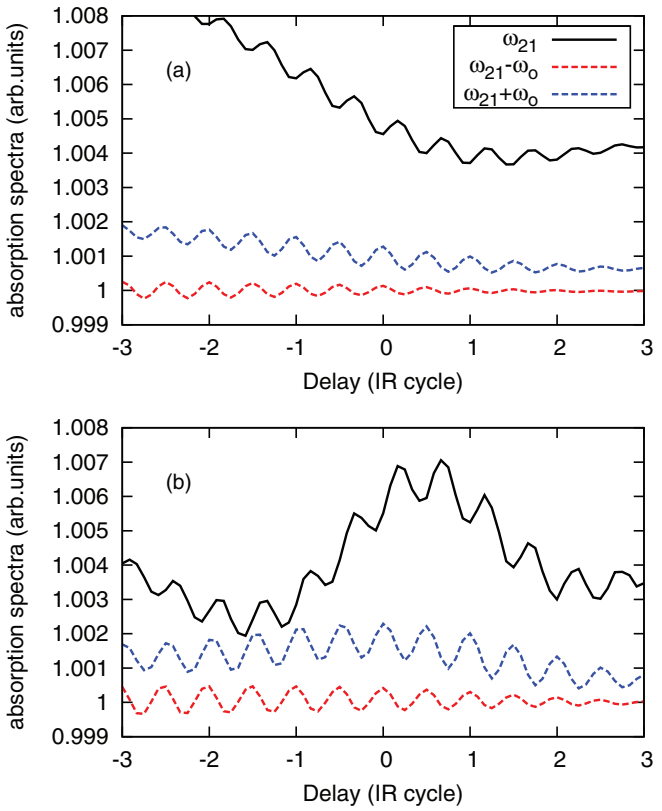

FIG. 6. (Color online) The segment of absorption spectra in Fig. 5 along the $1s$-$2p$ transition line (ω_{21}) and the sidebands at $\omega_{21} \pm \omega_o$ for peak IR-field intensities of (a) 1 TW cm^{-2} and (b) 5 TW cm^{-2}. In both cases, the XUV absorption spectra and their sidebands are modulating with opposite phases.

sidebands $\omega_{21} \pm \omega_o$ of Figs. 5(a) and 5(b) in Fig. 6. We find that the IR-photon absorption takes place at the zero crossing of the IR field when the momentum transfer from the field to the electron is maximum. A similar effect is known for the laser-driven ionization assisted by a train of attosecond pulses [18,19].

In Fig. 5, the dressed-state sidebands and the dynamical ac shifts disappear from absorption spectra long before the end of the IR envelope. This means that the IR field was not strong enough to dress or couple the excited states after they had been created by the XUV pulse beyond a certain delay time. The sharp delay-dependent sidebands near the $1s$-$2p$ transition line at the beginning of the IR envelope are caused by the so-called perturbed free-induction decay [20]. These findings are consistent with the TDSE-based calculation for the helium atom in Ref. [4].

Furthermore, in Fig. 5(a), we observe the formation of AT doublets in both $1s$-$2p$ and $1s$-$3p$ absorption lines. The amount of splitting increases as the timing of the XUV pulse moves toward the peak of the IR-field envelope, and then decreases after it passes the peak. As noted in Sec. IV A, the separation of AT doublets for the $1s$-$2p$ transition in our calculation is three to four times larger than the prediction made by the three-level model. Contrary to the conventional three-level model (Sec. III A) which predicts larger AT splittings for higher n states, the splitting in Fig. 5(a) is smaller for the $1s$-$3p$ transition than for the $1s$-$2p$ transition. This may be due to the detuning caused by dynamical ac Stark shifts (cf. Sec. III B). Moreover, as the peak intensity of the IR field increases in Figs. 5(b) and 5(c), we observe multiple splittings, rather than doublets, in both $1s$-$2p$ and $1s$-$3p$ absorption lines; this could be a signature for coupling among the degenerate states [cf. Fig. 3(b)].

Figures 7 and 8 show absorption spectra with the 800 and 1600 nm (nonresonant) dressing fields, respectively. The AT doublets are absent, but the other features found for the resonant case in Fig. 5 are present in both figures, i.e., the half IR-cycle modulation of dressed-state sidebands and the

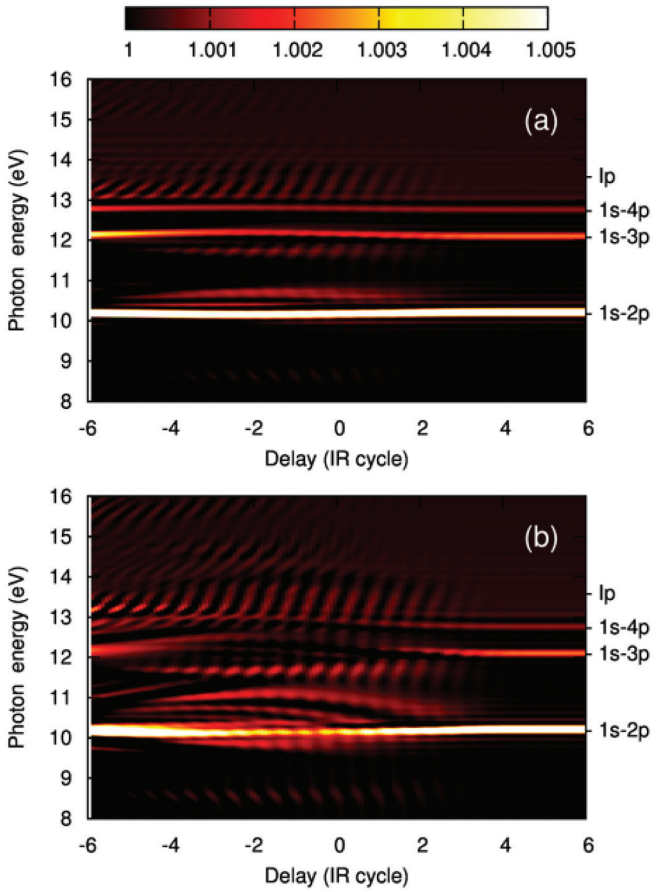

FIG. 7. (Color online) Absorption spectra of the hydrogen atom dressed with the 800 nm field of peak IR-field intensity (a) 1 TW cm^{-2} or (b) 5 TW cm^{-2}.

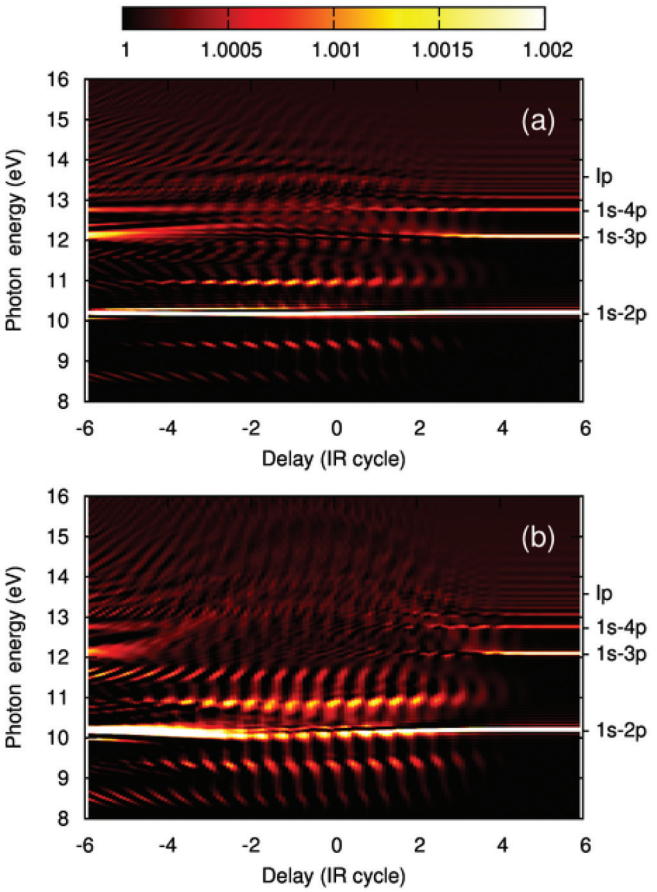

FIG. 8. (Color online) The same as Fig. 7 but with the 1600 nm dressing field.

appearance of multiple absorption lines for inner bound states. For the 1600 nm dressing field in particular, two additional features are worth mentioning. First, multiple sidebands appear between the $1s$-$2p$ and $1s$-$3p$ absorption lines, corresponding to the dressed states formed by one and two IR-photon absorptions. The separation between these sidebands is ω_o regardless of the intensity of the dressing laser field and the timing of the XUV pulse. Second, the large ponderomotive shift near the ionization threshold (cf. Sec. III B) is beautifully captured in Fig. 8(b).

In comparison with the three-level calculation in Ref. [8], our TDSE calculation supports their finding that including the nonadiabatic change in field strengths reproduces the half-cycle modulation of absorption spectra as observed in experiments. Yet, the multiple splittings of the 1-2 absorption line they found, as opposed to the AT doublet predicted by the RWA, remain questionable because the dressing IR-field intensity used in Ref. [8] is somewhat too high ($\sim 10^{14}$ W cm^{-2}) for atoms, which would induce ionization and rescattering to contaminate the absorption spectra. We do observe the multiple splitting of $1s$-$2p$ absorption lines in our results using smaller intensities ($\sim$TW cm^{-2}), e.g., Figs. 5(b), 5(c), and 7(b), but they are not symmetric around the unperturbed absorption line as in Ref. [8] but upshifted; it is not clear therefore if these multiple splittings are caused simply by relaxation of the RWA, or by removal of the degeneracy due to dressing fields.

C. Manipulation of absorption spectra

Finally, we consider the case where an IR field is linearly chirped, i.e.,

$$E_{\rm IR}(t) = E_0^{\rm (IR)}(t)\sin[q(\omega_o + bt)t]. \tag{20}$$

Figure 9 shows the effect of a linear chirp in the 1600 nm dressing field on the transient absorption spectra. The chirp rate is $b = -20$ meV/fs. As a result, the separation of sidebands is linearly decreasing in time, which is probed by the sweeping XUV pulse at a subcycle time scale. Such a manipulation of dressed states should be possible experimentally, as the chirped IR field is used routinely in the production of attosecond pulse trains [21,22].

V. CONCLUSION

To summarize, we studied the transient absorption spectra of an attosecond XUV pulse by laser-dressed hydrogen atoms. The sideband whose separation from the XUV absorption line is one IR-photon energy signifies a dressed state. Our calculation showed that dressed states are formed only if the timing of the XUV pulse is sufficiently early in the IR-field envelope, so that the subsequent interaction with the IR field is intense enough to dress the atom. Moreover, the population of dressed states was found to modulate with the XUV delay time; it is maximized if the XUV pulse is applied at the zero crossing of the IR field. These findings for dressed-state sidebands

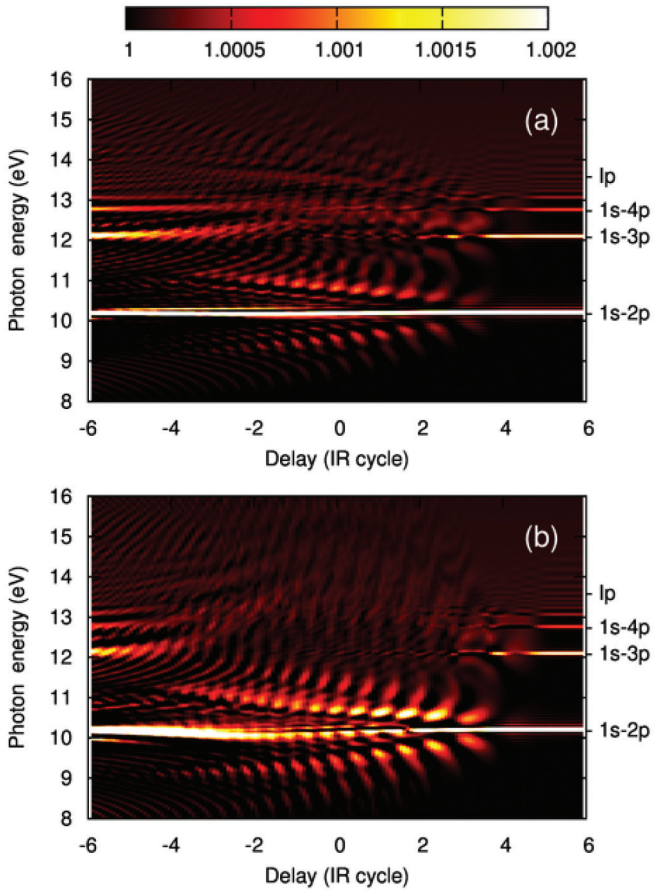

FIG. 9. (Color online) The same as Fig. 8 but with a negative linear chirp in the dressing field.

are consistent with the experiments for the helium atom in Refs. [3,4].

In transient absorption spectroscopy, dynamical ac Stark shifts of bound-state energies are induced by an IR field and measured by XUV pulses. We observed the multiple splitting of the XUV absorption line for inner p states while the atom was dressed with the IR field, with both resonant and nonresonant IR fields. Unlike the energy of dressed states, which is fixed by an amount of one IR-photon energy, the separation of these splittings changes in response to the IR envelope. They can be interpreted as the dynamical ac Stark shifts caused by the coupling among various degenerate states in the hydrogen atom. In addition, for weak resonant IR fields in particular, the AT doublets appeared in our spectra as expected, but the amount of their splitting was not in agreement with the prediction made by the conventional three-level model that neglects the dynamical ac Stark shifts. Lastly, we demonstrated that it is possible to manipulate the energy of dressed states at a subcycle time scale by using the chirped IR field.

ACKNOWLEDGMENTS

This work was partially supported by the U.S. Department of Energy. We also would like to acknowledge the partial support of the National Science Council of Taiwan and National Taiwan University (Grants No. 102R104021 and No. 102R8700-2).

APPENDIX

Hamiltonian of the three-level system in bichromatic fields is given by [23]

$$\mathcal{H}(t) = \mathcal{H}_0 + \sum_i V_i(t) \quad (i = 1,2), \tag{A1}$$

where

$$\mathcal{H}_0|\alpha\rangle = E_\alpha|\alpha\rangle \quad (\alpha = 1,2,3), \tag{A2}$$

$$V_i(t) = \sqrt{I_i}z\,\cos(\omega_i t + \phi_i). \tag{A3}$$

It is assumed that levels $|1\rangle$ and $|3\rangle$ have the same parity, whereas $|2\rangle$ has the opposite parity. In the interaction picture, and in the limit of the RWA, it becomes

$$\mathcal{H}_{\rm RWA} = \begin{bmatrix} 0 & \Omega_{12}^{(1)} & 0 \\ \Omega_{12}^{(1)*} & \Delta_1 & \Omega_{23}^{(2)} \\ 0 & \Omega_{23}^{(2)*} & \Delta_1 + \Delta_2 \end{bmatrix}, \tag{A4}$$

where

$$\Omega_{\alpha\beta}^{(i)} = \frac{\sqrt{I_i}}{2}\langle\alpha|z|\beta\rangle, \tag{A5}$$

$$\Delta_1 = (E_2 - E_1) - (2n_1 + 1)\omega_1 \quad (n_1 = 0,1,2,\ldots), \tag{A6}$$

$$\Delta_2 = (E_3 - E_2) - (2n_2 + 1)\omega_2 \quad (n_2 = 0,1,2,\ldots). \tag{A7}$$

On the other hand, the Floquet Hamiltonian of the system is given by [24]

$$\mathcal{H}_F = \begin{bmatrix} \delta_1 & A & \gamma \\ A^* & \Delta_1 + \delta_2 & B \\ \gamma^* & B^* & \Delta_1 + \Delta_2 + \delta_3 \end{bmatrix}, \tag{A8}$$

where

$$\delta_1 = -\left|\Omega_{12}^{(1)}\right|^2 \left\{\frac{1}{(2n_1+2)\omega_1} + \Theta(n_1)\frac{1}{2n_1\omega_1}\right\} - \left|\Omega_{12}^{(2)}\right|^2 \left\{\frac{1}{(2n_1+1)\omega_1 + \omega_2} + \frac{1}{(2n_2+1)\omega_1 - \omega_2}\right\}, \tag{A9}$$

$$\delta_3 = \left|\Omega_{23}^{(1)}\right|^2 \left\{\frac{1}{\omega_1 + (2n_2+1)\omega_2} + \frac{1}{-\omega_1 + (2n_2+1)\omega_2}\right\} + \left|\Omega_{23}^{(2)}\right|^2 \left\{\frac{1}{(2n_2+2)\omega_2} + \Theta(n_2)\frac{1}{2n_2\omega_2}\right\}, \tag{A10}$$

$$\delta_2 = -(\delta_1 + \delta_3), \tag{A11}$$

with

$$\Theta(n) \equiv \begin{cases} 0 & \text{if } n = 0 \\ 1 & \text{otherwise,} \end{cases} \tag{A12}$$

and

$$A = \frac{(-1)^{n_1}\left(\Omega_{12}^{(1)}\right)^{2n_1+1}\exp[-i(2n_1+1)\phi_1]}{2^{2n_1}(n_1!)^2{\omega_1}^{2n_1}}, \tag{A13}$$

$$B = \frac{(-1)^{n_2}\left(\Omega_{23}^{(2)}\right)^{2n_2+1}\exp[-i(2n_2+1)\phi_2]}{2^{2n_2}(n_2!)^2{\omega_2}^{2n_2}}. \tag{A14}$$

In general, γ is negligibly small for multiphoton ($n_1 > 0$ or $n_2 > 0$) transitions. For the two-photon resonance ($n_1 = 0$ and $n_2 = 0$), it is given by

$$\gamma = \frac{\Omega_{12}^{(2)}\Omega_{23}^{(1)}}{\omega_2 - \omega_1}. \tag{A15}$$

If $A \ll B$, then one can perform the following unitary transformation to partially diagonalize $\mathcal{H}_F$:

$$\tilde{\mathcal{H}}_F = S^{-1}\mathcal{H}_F S = \begin{bmatrix} \lambda_1 & u_2 & u_3 \\ u_2^* & \lambda_2 & 0 \\ u_3^* & 0 & \lambda_3 \end{bmatrix}, \tag{A16}$$

where

$$S = \begin{bmatrix} 1 & 0 & 0 \\ 0 & [(q+d)/2q]^{1/2} & B\,[2q(q+d)]^{-1/2} \\ 0 & -B^*\,[2q(q+d)]^{-1/2} & [(q+d)/2q]^{1/2} \end{bmatrix}, \tag{A17}$$

with

$$q = \sqrt{d^2 + |B|^2}, \tag{A18}$$

$$d = \frac{\Delta_2 - \delta_2 + \delta_3}{2}, \tag{A19}$$

and

$$\lambda_1 = \delta_1, \tag{A20}$$

$$\lambda_2 = \Delta_1 + \delta_2 + d - q, \tag{A21}$$

$$\lambda_3 = \Delta_1 + \delta_2 + d + q, \tag{A22}$$

$$u_2 = \frac{A(q+d) - \gamma B^*}{\sqrt{2q(q+d)}}, \tag{A23}$$

$$u_3 = \frac{AB + \gamma(q+d)}{\sqrt{2q(q+d)}}. \tag{A24}$$

The location of Autler-Townes doublets is then given by

$$\omega_{12}^{(k)} = \frac{(E_2 + \delta_2) - (E_1 + \delta_1) + \Delta_1 + \delta_1^{(k)} - \lambda_k}{2n_1 + 1} \quad (k = 2,3), \tag{A25}$$

where

$$\delta_1^{(2)} = \frac{|u_2|^2}{\lambda_1 - \lambda_2}, \tag{A26}$$

$$\delta_1^{(3)} = \frac{|u_3|^2}{\lambda_1 - \lambda_3}. \tag{A27}$$

Therefore, the amount of their splitting is

$$\Delta\varepsilon = \left|\omega_{12}^{(2)} - \omega_{12}^{(3)}\right| = \frac{\left|2q + \delta_1^{(2)} - \delta_1^{(3)}\right|}{2n_1 + 1}. \tag{A28}$$

[1] E. Goulielmakis, Z.-H. Loh, A. Wirth, R. Santra, N. Rohringer, V. S. Yakovlev, S. Zherebtsov, T. Pfeifer, A. M. Azzeer, M. F. Kling, S. R. Leone, and F. Krausz, Nature (London) **466**, 739 (2010).

[2] H. Wang, M. Chini, S. Chen, C.-H. Zhang, Y. Cheng, F. He, Y. Wu, U. Thumm, and Z. Chang, Phys. Rev. Lett. **105**, 143002 (2010).

[3] M. Chini, B. Zhao, H. Wang, Y. Cheng, S. X. Hu, and Z. Chang, Phys. Rev. Lett. **109**, 073601 (2012).

[4] S. Chen, M. J. Bell, A. R. Beck, H. Mashiko, M. Wu, A. N. Pfeiffer, M. B. Gaarde, D. M. Neumark, S. R. Leone, and K. J. Schafer, Phys. Rev. A **86**, 063408 (2012).

[5] X. M. Tong and N. Toshima, Phys. Rev. A **81**, 063403 (2010).

[6] R. Santra, V. S. Yakovlev, T. Pfeifer, and Z.-H. Loh, Phys. Rev. A **83**, 033405 (2011).

[7] M. B. Gaarde, C. Buth, J. L. Tate, and K. J. Schafer, Phys. Rev. A **83**, 013419 (2011).

[8] A. N. Pfeiffer and S. R. Leone, Phys. Rev. A **85**, 053422 (2012).

[9] W.-C. Chu and C. D. Lin, Phys. Rev. A **85**, 013409 (2012).

[10] M. Haas, U. D. Jentschura, C. H. Keitel, N. Kolachevsky, M. Herrmann, P. Fendel, M. Fischer, T. Udem, R. Holzwarth, T. W. Hänsch, M. O. Scully, and G. S. Agarwal, Phys. Rev. A **73**, 052501 (2006).

[11] K. Ishikawa and K. Midorikawa, Phys. Rev. A **65**, 031403(R) (2002).

[12] X. M. Tong, P. Ranitovic, C. L. Cocke, and N. Toshima, Phys. Rev. A **81**, 021404(R) (2010).

[13] X.-M. Tong and S.-I. Chu, Chem. Phys. **217**, 119 (1997).

[14] M. Freischhauer, A. Imamoglu, and J. P. Marangos, Rev. Mod. Phys. **77**, 633 (2005).

[15] D. H. Kobe, J. Phys. B **16**, 1159 (1983).

[16] B. J. Sussman, Am. J. Phys. **79**, 477 (2011).

[17] S.-I. Chu and J. Cooper, Phys. Rev. A **32**, 2769 (1985).

[18] P. Johnsson, J. Mauritsson, T. Remetter, A. L'Huillier, and K. J. Schafer, Phys. Rev. Lett. **99**, 233001 (2007).

[19] P. Ranitovic, X. M. Tong, C. W. Hogle, X. Zhou, Y. Liu, N. Toshima, M. M. Murnane, and H. C. Kapteyn, Phys. Rev. Lett. **106**, 193008 (2011).

[20] C. H. B. Cruz, J. P. Gordon, P. C. Becker, R. L. Fork, and C. V. Shank, IEEE J. Quantum Electron. **24**, 261 (1988).

[21] J. Mauritsson, P. Johnsson, R. López-Martens, K. Varjú, W. Kornelis, J. Biegert, U. Keller, M. B. Gaarde, K. J. Schafer, and A. L'Huillier, Phys. Rev. A **70**, 021801 (2004).

[22] M. Murakami, J. Mauritsson, A. L'Huillier, K. J. Schafer, and M. B. Gaarde, Phys. Rev. A **71**, 013410 (2005).

[23] T.-S. Ho and S.-I. Chu, Phys. Rev. A **31**, 659 (1985).

[24] K. Wang, T.-S. Ho, and S.-I. Chu, J. Phys. B **18**, 4539 (1985).